SLAC-PUB-2247
January 1979
(T/E)

QUARK STRUCTURE FUNCTIONS OF MESONS AND THE DRELL-YAN PROCESS*

Edmond L. Berger** and Stanley J. Brodsky
Stanford Linear Accelerator Center
Stanford University, Stanford, California 94305

ABSTRACT

The polarization properties and longitudinal momentum distribution of massive lepton pairs produced in hadronic collisions are shown to depend in detail on the internal dynamics of the incident hadrons. For meson-induced reactions, we use QCD perturbation theory to predict that at small transverse momentum of the pair, the decay angular distribution in the pair rest frame will change from predominantly $1+\cos^2\theta$ to $\sin^2\theta$ as the longitudinal momentum fraction of the pair $x_F \to +1$. The two angular distributions are associated respectively with $(1-x)^2$ and $Q^{-2}(1-x)^0$ components of the valence quark structure function of the meson.

(Submitted to Physical Review Letters)

---

* Work supported by the Department of Energy under contract number EY-76-C-03-0515.

** Permanent address: High Energy Physics Division, Argonne National Laboratory.

The Drell-Yan process[1] $A+B \to \ell\bar{\ell}X$ measures the ability of colliding hadrons to reconfigure their momentum into the local production of a massive lepton pair with four-momentum Q^μ. As the edge of phase space is approached (i.e., $\tau = Q^2/s \to 1$ or $x_F = Q_L/Q_L^{max} \to 1$), an annihilating quark q or anti-quark $\bar{q}$ in the subprocess $\bar{q}q \to \gamma^* \to \ell\bar{\ell}$ is taken far off-shell, and consequently the far off-shell short distance internal dynamics of the hadronic wave function is probed. The Drell-Yan process can thus be used to determine the structure functions of hadrons not normally accessible in deep inelastic scattering and to measure other important aspects of the dynamics (e.g., spin properties) of the hadronic constituents at short distance.

In this letter, we report an analysis of meson-induced massive lepton pair production $MB \to \ell^+\ell^-X$ in the context of perturbative quantum chromodynamics (QCD). We go beyond the usual treatments by including explicit effects associated with the meson bound state.[2] We assume that in the low momentum transfer domain, the meson wave function describes a $q\bar{q}$ bound state, and that at large momentum transfer, the momentum dependence of the meson wave function is controlled by the Bethe-Salpeter kernel -- and thus by single gluon exchange in the asymptotic freedom limit. This idea is sketched in Fig. 1. The same model[3] yields the standard predictions[3,4] for the power behavior of meson and baryon form factors at large Q^2, and for baryon valence structure functions, all consistent with experiment. Our focus here is on the consequences of the QCD description of internal hadron dynamics; logarithmic corrections due to QCD radiative processes can be treated in the conventional manner.

The most striking testable consequences of this QCD picture for $MB \to \ell^+\ell^- X$ are its predictions for the valence quark structure function of the meson and for the polarization of the virtual photon $\gamma^* \to \ell^+\ell^-$. The structure function has both a scaling[5] $(1-x)^2$ and a non-scaling[6] $Q^{-2}(1-x)^0$ component, with specified relative magnitude. Each is associated with a different angular distribution in the lepton pair rest frame. For $Mq \to \ell^+\ell^- X$, we obtain

$$d\sigma \propto (1-x)^2 (1+\cos^2\theta) + \frac{4}{9} \frac{\overline{k_T^2}}{Q^2} \sin^2\theta \quad . \qquad (1)$$

Here x is the momentum fraction (light-cone variable) of the annihilating $\bar{q}$ from the meson, $\overline{k_T^2}$ is the average of its squared transverse momentum, and $\cos\theta = \hat{p}_\ell \cdot \hat{p}_\pi$ is defined in the lepton pair rest frame. Identification of the non-scaling piece in the data can be made in several different ways: the x dependence of the cross section at fixed Q^2,s; the angular (θ) dependence at fixed x,Q^2,s; and s dependence at fixed Q^2/s.

The dominant contribution to $\pi^- N \to \mu^+\mu^- X$ at large Q^2 arises from the annihilation $\bar{u}u \to \gamma^* \to \mu^+\mu^-$, where the antiquark $\bar{u}$ comes from the π^- and u from the nucleon. We concentrate on the kinematic region where only the $\bar{u}$ is far off-shell (i.e., $x_F \to 1$). It is sufficent to treat the u quark as nearly free and on-shell. Thus, the incident nucleon structure is not indicated in the lowest order diagrams shown in Fig. 1 for $\pi^- q \to \gamma^* q$. Both diagrams in Fig. 1 are required by gauge invariance, although in a physical (axial) gauge, the scaling contributions as $Q^2 \to \infty$ can be identified solely with Fig. 1(a). We partition the incident meson momentum p equally between the constituent q and $\bar{q}$; this simplifying approximation can be discarded as it does not affect our conclusions.

The kinematics of the annihilating antiquark are specified with light-cone variables $x_a = (p_a^0 + p_a^3)/(p^0 + p^3)$, and k_{Ta}. Setting $p_1^2 = m^2$, where m denotes the bare quark mass, we use energy and momentum conservation to derive

$$p_a^2 = -\frac{\vec{k}_{Ta}^2 + x_a m^2 - x_a(1-x_a)\, m_\pi^2}{(1-x_a)} \quad . \tag{2}$$

As $x_a \to 1$, p_a^2 becomes large and far space-like. The squared four momentum carried by the gluon in Fig. 1, $k^2 = (p_1 - \tfrac{1}{2}p)^2 = \tfrac{1}{2}(p_a^2 + m^2) - \tfrac{1}{4}m_\pi^2$, also becomes large as $x_a \to 1$. Therefore, invoking arguments based on asymptotic freedom, we suppose that in the range of x_a of interest to us, the single gluon exchange approximation shown in Fig. 1 will yield a good representation of the asymptotic large momentum behavior of the Bethe-Salpeter kernel for the $q\bar{q}$ bound state.[7]

The invariant amplitude corresponding to Fig. 1 is

$$\mathcal{M} \propto \bar{u}(p_+)\, \gamma_\mu\, v(p_-)\, \frac{1}{Q^2}\, \frac{\alpha_s(k^2)}{k^2}\, \psi_\pi(\vec{0})$$

$$\sum_\lambda \bar{u}(p_1)\, \gamma_\alpha\, u_\lambda(p/2)\, \bar{v}_{-\lambda}(p/2)$$

$$\left[-\gamma^\alpha \frac{1}{\not{p}_a + m}\, \gamma^\mu + \gamma^\mu \frac{1}{\not{p}_c - m}\, \gamma^\alpha\right] u(p_b) \quad , \tag{3}$$

where $\sum_\lambda u_\lambda \bar{v}_{-\lambda} = (\tfrac{1}{2}\not{p} + m)\, \gamma_5$ specifies that the $\bar{u}d$ bound state is a pseudoscalar.[8] The factor $\psi_\pi(\vec{r} = \vec{0})$ in Eq. (3) represents an integration over the soft momenta in the pion wave function. We remark that our expression for the amplitude is precisely correct in the limit of zero binding energy for the meson. Note also that in our calculation the

quark transverse momentum $\vec{k}_T$ enters explicitly; it is not an arbitrarily assigned "intrinsic" or "primordial" $\vec{k}_T$ associated with the $q\bar{q}$ binding in the wave function.

For simplicity in what follows, we set $m^2 = 0$ and $m_\pi^2 = 0$, and we restrict our attention to $\vec{k}_{Ta}^2 \ll Q^2$. Using the amplitude in Eq. (3), we compute an explicit expression for the cross section for $\pi^- N \to \mu\bar{\mu}X$. After integration over the azimuthal angle in the pair rest frame, we obtain

$$\frac{Q^2\, d\sigma}{dQ^2\, d^2\vec{Q}_T\, dx_L\, d\cos\theta} \propto \int d^2\vec{k}_{Ta}\, dx_a\, d^2 k_{Tb}\, dx_b\, G_{q/N}(x_b, \vec{k}_{Tb}) \frac{\psi_\pi^2(0)}{k_{Ta}^4}\left[(1-x_a)^2(1+\cos^2\theta) + \frac{4}{9}\frac{k_{Ta}^2}{Q^2}\sin^2\theta\right] \delta^{(2)}(\vec{Q}_T - \vec{k}_{Ta} - \vec{k}_{Tb})\ \delta(x_L - x_a - x_b)\ \delta(Q^2 - x_a x_b s)\ . \tag{4}$$

Here $G_{q/N}$ is the quark structure function of the nucleon. We have discarded contributions which are of order $Q^{-2}k_T^2(1-x_a)$ and $Q^{-4}k_T^4(1-x_a)^{-1}$ in the square brackets of Eq. (4).[9] The contributions from sea quarks and antiquarks in the meson and nucleon are also ignored in Eq. (4).

In the Bjorken scaling limit, $Q^2 \to \infty$, at fixed x_a, the valence quark structure function can be extracted from Eq. (4):

$$G_{\bar{q}/\pi}(x) = \int d^2\vec{k}_T\, G_{\bar{q}/\pi}(x, \vec{k}_T) \propto (1-x)^2\ . \tag{5}$$

The corresponding $\vec{k}_T$ fall-off produces pairs with a Q_T^{-4} distribution[2] (for $k_{Ta}^2 \ll Q^2$).

We observe the following additional features of Eq. (4):

(i) We can identify a non-scaling contribution to the structure function. After averaging over $\cos\theta$, we obtain:

$$G_{\bar{q}/\pi} \to (1-x)^2 + \frac{2}{9}\frac{\overline{k_T^2}}{Q^2} \quad . \tag{6}$$

The non-scaling contribution is independent of x and will dominate the scaling contribution at fixed $Q^2(1-x)$ as $Q^2 \to \infty$. In our model the relative magnitude of the scaling and non-scaling terms is fixed.[9] When the non-scaling term dominates in Eq. (4), the mean $\overline{k_{Ta}^2}$ is of order $Q^2/\log Q^2$.

(ii) The non-scaling contribution corresponds to a longitudinal structure function and provides a $\sin^2\theta$ angular distribution in the lepton pair rest frame, in contrast to the conventional expectation of $(1+\cos^2\theta)$. At fixed Q^2, the $\sin^2\theta$ term dominates in the cross section as $x_F \to 1$. The usual rule that annihilating spin -1/2 quarks produce transversely polarized photons is modified when off-shell constituents are involved. In our case, the $\bar{q}$ is kinematically far off-shell since, as $x_F \to 1$, all of the momentum of the recoil spectator quark must be transfered to the annihilation subprocess. In this situation the spin of the incident meson influences the final angular distribution. In a different language, the bound state effect can be identified with a "high-twist" subprocess, since more than the minimum number of elementary fields is required.

In the range $4.0 \leq M = (Q^2)^{1/2} \leq 8.5$ GeV, an effective pion structure function has been extracted by the Chicago-Princeton collaboration[10] from their data on $\pi^- N \to \mu^+\mu^- X$ at 225 GeV/c. They report that $xG_\pi^{expt}(x)$

$\simeq 0.5\ (1-x)^{1.01 \pm 0.05}$ for $x > 0.3$. For similar values of Q^2, our structure function in Eq. (6) can mimic the observed $(1-x)^1$ behavior if we choose $\overline{k_T^2} \simeq 1\ \text{GeV}^2$. This value of $\overline{k_T^2}$ is consistent with measured[10] values of $\langle Q_T^2 \rangle = \langle (\vec{k}_{Ta} + \vec{k}_{Tb})^2 \rangle$. We remark parenthetically that the parameter $\overline{k_T^2}$ in our formulas is a function of Q^2 and x and effectively includes the mass terms which were dropped when we set m^2 and $m_\pi^2 = 0$. Shown in Fig. 2(a) is a comparison of our structure function, Eq. (6), for different values of Q^2, with the form $G_\pi^{expt}(x)$ deduced from the data, assuming Q^2 independence. We urge that the analysis of the data be repeated with Eq. (6).

In Fig. 2(b) we present our prediction for the polarization parameter α in the expression $d\sigma/d\cos\theta = 1 + \alpha\cos^2\theta$. In our model, $\alpha = (1-r)/(1+r)$, with

$$r = \frac{4}{9} \frac{\overline{k_{Ta}^2}}{Q^2(1-x_a)^2} \quad . \tag{7}$$

Our predictions are presented as a function $x_F = (x_a - \tau/x_a)/(1-\tau)$. The angle θ is referred to the t-channel (or Gottfried-Jackson) system of axes: $\cos\theta = \hat{p}_\mu \cdot \hat{p}_\pi$. Observed values of α are reported[10] only for data averaged over all x_F, and, as we expect in this case, $\alpha \simeq 1$ for $4 < M < 8.5$ GeV.

The experimental observation of an effective $(1-x)^1$ behavior of the quark structure function of the pion is incompatible with general crossing arguments for Born diagrams which mandate only even powers of $(1-x)$ as $x \to 1$ when a fermion is extracted from a meson.[11] The linear behavior $(1-x)$ would be expected or <u>spinless</u> quarks. On the other hand, the spin-1/2 nature of the constituents seems well established by the observation in

the same experiment of a decay angular distribution of $1+\alpha\cos^2\theta$ with $\alpha \simeq 1$. Our analysis provides a resolution of this apparent paradox. We suggest that the observed $(1-x)^1$ behavior is an approximation to our Eq. (6), in which only even powers of $(1-x)$ appear. The critical test of this assertion is the identification of the predicted $\sin^2\theta$ behavior of the decay angular distribution at large x_F.

Observation of our predicted $\sin^2\theta$ non-scaling term in the data would reinforce the applicability of the Drell-Yan model with spin-1/2 quarks and verify that structure functions can be understood in some detail in a QCD framework. Failure would mean that there is no fundamental explanation for the observed power behavior of structure functions. The non-scaling and angular dependent effects we derive are in addition to, but much stronger than analogous effects provided by QCD gluonic radiative corrections; in particular, our prediction for the angular distribution applies at small Q_T, where gluonic radiative corrections do not upset the conventional $1 + \cos^2\theta$ expectation.[12] The form we derive for the structure function in Eq. (6) should apply universally; for example, an analogous structure function should also be observed in meson induced large p_T hadronic processes.[13]

In baryon (or antibaryon) induced reactions, $BB \to \ell\bar{\ell}X$, the $1 + \cos^2\theta$ behavior characteristic of spin-1/2 systems is maintained as $x \to 1$. However, non-scaling longitudinal contributions arise near $x = 2/3$ if we take into account the subprocess $(qq) + \bar{q} \to q + \gamma^*$ with a bosonic diquark system.[14] These effects may be related to the anomalous values of σ_L/σ_T observed in deep inelastic electron scattering[15] at moderate values of Q^2.

ACKNOWLEDGEMENT

We thank R. Blankenbecler for helpful conversations.

REFERENCES

1. S. D. Drell and T. M. Yan, Phys. Rev. Lett. 25, 316 (1970); 25, 902 (1970). For a recent review see E. L. Berger, Proceedings of the 1978 Vanderbilt Conference, AIP Conference Proceedings Series, No. 45, Ed. by R. S. Panvini and S. E. Csorna.

2. M. Duong-van, K. V. Vasavada and R. Blankenbecler, Phys. Rev. D16, 1389 (1977); C. Debeau and D. Silverman, SLAC-PUB-2187 (Aug. 1978).

3. S. J. Brodsky and G. R. Farrar, Phys. Rev. Lett. 31, 1153 (1973) and Phys. Rev. D11, 1309 (1975).

4. V. A. Matveev, R. M. Muradyan and A. N. Tavkheldize, Lett. Nuovo Cimento 7, 719 (1973).

5. Z. F. Ezawa, Nuovo Cimento 23A, 271 (1974).

6. G. R. Farrar and D. R. Jackson, Phys. Rev. Lett. 35, 1416 (1975). Our results are analogous to those for $e^+e^- \to \pi X$ derived by Farrar and Jackson. However, in the Drell-Yan process, the dominance of the longitudinal term at large x cannot be attributed to exclusive channels. See also A. I. Vainshtain and V. I. Zakharov, Phys. Lett. 72B, 368 (1978).

7. See, e.g., T. Appelquist and E. Poggio, Phys. Rev. D10, 3280 (1974) and Ref. 3. A detailed discussion will be given by S. J. Brodsky

and P. Lepage (to be published). For a similar problem in QED, see W. Caswell and P. Lepage, Phys. Rev. A18, 810 (1978).

8. Our results also hold when the quark spins are uncorrelated.

9. Our results are accurate in two $Q^2 \to \infty$ limits: (a) the fixed x_a Bjorken limit, and (b) the fixed $W^2 = (1-x)Q^2/x$ limit, with $W^2 >> \vec{k}_T^2$. The neglected terms in Eq. (4) must be retained at modest Q^2 for x very close to 1 (> 0.95).

10. K. J. Anderson et al., Chicago-Princeton Report EFI-78-38 submitted to the XIX International Conference on High Energy Physics, Tokyo; and private communications.

11. S. D. Drell, D. J. Levy and T. M. Yan, Phys. Rev. D1, 1617 (1970). For a discussion of non-Born diagrams, see P. V. Landshoff and J. C. Polkinghorne, Phys. Rev. D6, 3708 (1972).

12. K. Kajantie, J. Linfors and R. Raitio, Phys. Lett. 74B, 384 (1978); E. L. Berger, J. T. Donohue and S. Wolfram, Phys. Rev. D17, 858 (1978); and E. Berger, Ref. 1.

13. A measurement of the quark structure function of the pion as seen in pion induced hadronic jets is reported by the Pennsylvania-Wisconsin Collaboration, M. Dris et al., Reports UPR-39E (Rev.) and UPR-55E (1978).

14. In deep-inelastic processes, $\gamma^* + (qq)$ subprocesses have been considered by I. A. Schmidt, SLAC Report 203, 1977 (Ph.D. Thesis); I. A. Schmidt and R. Blankenbecler, Phys. Rev. D16, 1318 (1977).

15. E. M. Riordan et al., Phys. Rev. Lett. 33, 561 (1974); R. E. Taylor, Proceedings Symposium on Lepton and Photon Interactions at High Energies, Stanford, 1975; W. B. Atwood, SLAC Report 185 (June 1975).

FIGURE CAPTIONS

1. Diagrams for $Mq \to q\gamma^*$, $\gamma^* \to \mu^+\mu^-$. Solid single lines represent quarks. Symbols p_1, p_a, p_b, and p_c denote four-momenta of quarks and k is the four-momentum of the gluon.

2. (a) The quantity $xq_\pi(x)$ is presented as a function of x for two values of Q^2 near the top and bottom of the range explored experimentally. Here we set $xq_\pi(x) = 2xG_{\bar{q}/\pi}$ with $G_{\bar{q}/\pi}$ provided in Eq. (6), and $\overline{k_T^2} = 1\ \text{GeV}^2$. The factor 2 is chosen to reproduce approximately the normalization of the experimentally deduced effective $xq_\pi(x)$ near $x = 0.5$. For comparison, we plot as a dashed curve the experimental form (Ref. 10) $0.5\ (1-x)^{1.01}$. The computations in this paper are applicable only for $x > 0.5$.

   (b) Predicted value of α as a function of x_F for different values of $M\ (= (Q^2)^{1/2})$ at $p_{lab} = 225$ GeV/c, with $\overline{k_T^2} = 1\ \text{GeV}^2$.

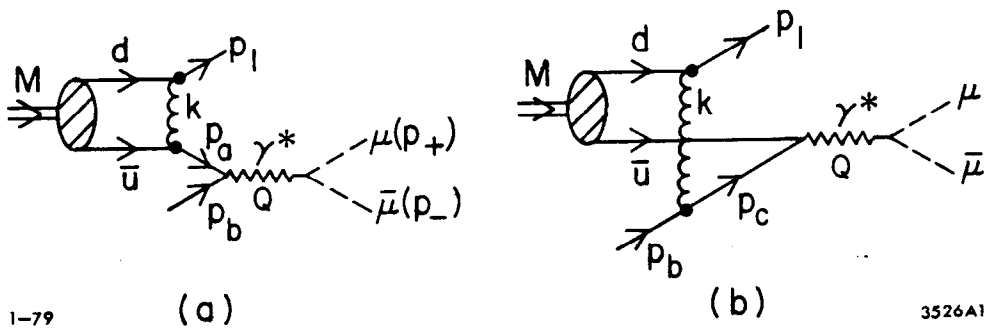
M
d
p_l
k
p_a
γ^*
$\mu(p_+)$
$\bar{u}$
Q
$\bar{\mu}(p_-)$
p_b
(a)
M
d
p_l
k
γ^*
μ
$\bar{u}$
Q
$\bar{\mu}$
p_c
p_b
(b)
1–79
3526A1

Fig. 1

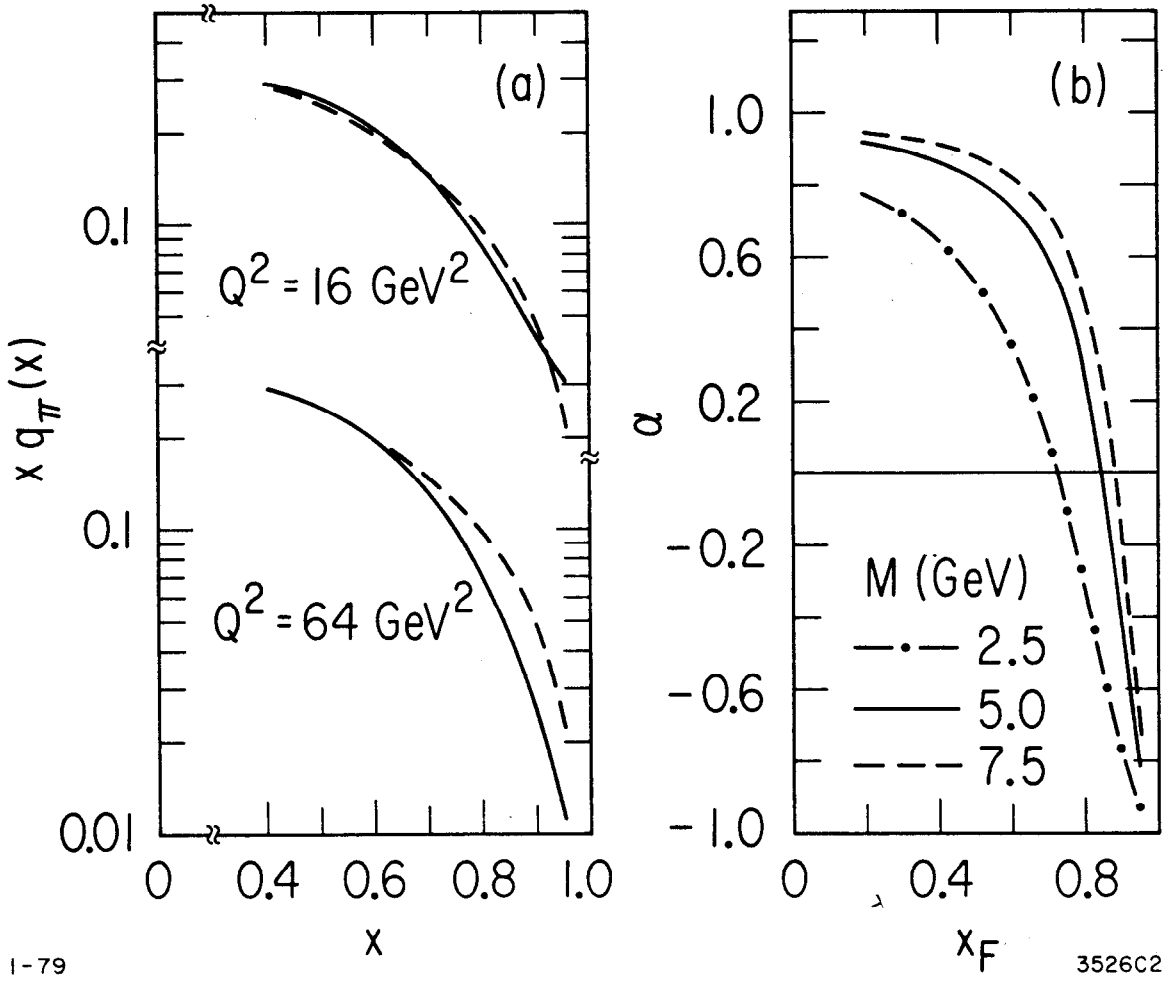
(a)
(b)
$Q^2 = 16$ GeV^2
$Q^2 = 64$ GeV^2
$x\, q_\pi(x)$
α
0.1
0.1
0.01
0
0.4
0.6
0.8
1.0
x
1.0
0.6
0.2
-0.2
-0.6
-1.0
0
0.4
0.8
x_F
M (GeV)
2.5
5.0
7.5
1-79
3526C2

Fig. 2